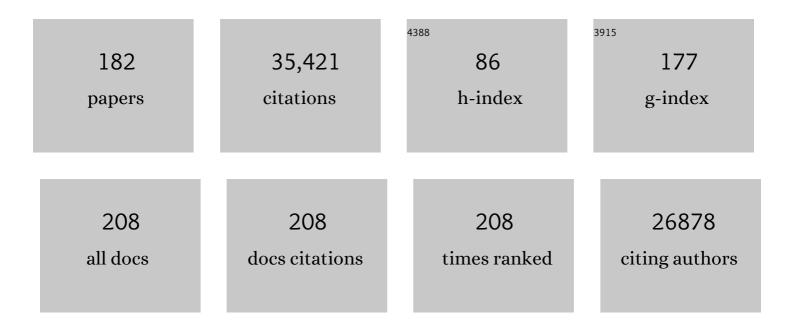
Stephen C Harrison

List of Publications by Year in descending order

Source: https://exaly.com/author-pdf/1060556/publications.pdf Version: 2024-02-01



#	Article	IF	CITATIONS
1	Recall of B cell memory depends on relative locations of prime and boost immunization. Science Immunology, 2022, 7, eabn5311.	11.9	20
2	Antibodies induced by an ancestral SARS-CoV-2 strain that cross-neutralize variants from Alpha to Omicron BA.1. Science Immunology, 2022, 7, eabo3425.	11.9	28
3	Antibodies That Engage the Hemagglutinin Receptor-Binding Site of Influenza B Viruses. ACS Infectious Diseases, 2021, 7, 1-5.	3.8	11
4	Recapitulation of HIV-1 Env-antibody coevolution in macaques leading to neutralization breadth. Science, 2021, 371, .	12.6	49
5	Functional refolding of the penetration protein on a non-enveloped virus. Nature, 2021, 590, 666-670.	27.8	33
6	Structural basis of Stu2 recruitment to yeast kinetochores. ELife, 2021, 10, .	6.0	11
7	Differential immune imprinting by influenza virus vaccination and infection in nonhuman primates. Proceedings of the National Academy of Sciences of the United States of America, 2021, 118, .	7.1	15
8	A Prevalent Focused Human Antibody Response to the Influenza Virus Hemagglutinin Head Interface. MBio, 2021, 12, e0114421.	4.1	17
9	Ctf3/CENP-I provides a docking site for the desumoylase Ulp2 at the kinetochore. Journal of Cell Biology, 2021, 220, .	5.2	4
10	Recognition of Divergent Viral Substrates by the SARS-CoV-2 Main Protease. ACS Infectious Diseases, 2021, 7, 2591-2595.	3.8	55
11	Memory B cell repertoire for recognition of evolving SARS-CoV-2 spike. Cell, 2021, 184, 4969-4980.e15.	28.9	94
12	Structure of the Vesicular Stomatitis Virus L Protein in Complex with Its Phosphoprotein Cofactor. Cell Reports, 2020, 30, 53-60.e5.	6.4	51
13	The Structural Basis for Kinetochore Stabilization by Cnn1/CENP-T. Current Biology, 2020, 30, 3425-3431.e3.	3.9	19
14	Structure of a nascent membrane protein as it folds on the BAM complex. Nature, 2020, 583, 473-478.	27.8	101
15	Structure of a rabies virus polymerase complex from electron cryo-microscopy. Proceedings of the National Academy of Sciences of the United States of America, 2020, 117, 2099-2107.	7.1	58
16	Cryoelectron Microscopy Structure of a Yeast Centromeric Nucleosome at 2.7ÂÃ Resolution. Structure, 2020, 28, 363-370.e3.	3.3	19
17	Cryo-EM Structure of Full-length HIV-1 Env Bound With the Fab of Antibody PG16. Journal of Molecular Biology, 2020, 432, 1158-1168.	4.2	47
18	The human dimension in contemporary biological research. Nature Structural and Molecular Biology, 2020, 27, 107-108	8.2	0

#	Article	IF	CITATIONS
19	Structures of the ATP-fueled ClpXP proteolytic machine bound to protein substrate. ELife, 2020, 9, .	6.0	105
20	Horaceâ \in ™s hymn to Bacchus (Odes 2.19): poetics and politics. , 2020, , 231-252.		2
21	Structure of the Centromere Binding Factor 3 Complex from Kluyveromyces lactis. Journal of Molecular Biology, 2019, 431, 4444-4454.	4.2	3
22	In situ Structure of Rotavirus VP1 RNA-Dependent RNA Polymerase. Journal of Molecular Biology, 2019, 431, 3124-3138.	4.2	45
23	Antibodies to a Conserved Influenza Head Interface Epitope Protect by an IgG Subtype-Dependent Mechanism. Cell, 2019, 177, 1124-1135.e16.	28.9	141
24	Autoreactivity profilesÂof influenza hemagglutinin broadly neutralizingÂantibodies. Scientific Reports, 2019, 9, 3492.	3.3	49
25	Affinity maturation in a human humoral response to influenza hemagglutinin. Proceedings of the National Academy of Sciences of the United States of America, 2019, 116, 26745-26751.	7.1	25
26	Self-tolerance curtails the B cell repertoire to microbial epitopes. JCI Insight, 2019, 4, .	5.0	32
27	The structure of the Ctf19c/CCAN from budding yeast. ELife, 2019, 8, .	6.0	71
28	The structure of the yeast Ctf3 complex. ELife, 2019, 8, .	6.0	15
29	Memory B Cells that Cross-React with Group 1 and Group 2 Influenza A Viruses Are Abundant in Adult Human Repertoires. Immunity, 2018, 48, 174-184.e9.	14.3	124
30	Conserved epitope on influenza-virus hemagglutinin head defined by a vaccine-induced antibody. Proceedings of the National Academy of Sciences of the United States of America, 2018, 115, 168-173.	7.1	113
31	Structure of the DASH/Dam1 complex shows its role at the yeast kinetochore-microtubule interface. Science, 2018, 360, 552-558.	12.6	72
32	HIV envelope V3 region mimic embodies key features of a broadly neutralizing antibody lineage epitope. Nature Communications, 2018, 9, 1111.	12.8	30
33	Kinetochore Function from the Bottom Up. Trends in Cell Biology, 2018, 28, 22-33.	7.9	50
34	Visualization of Calcium Ion Loss from Rotavirus during Cell Entry. Journal of Virology, 2018, 92, .	3.4	27
35	Structure of the membrane proximal external region of HIV-1 envelope glycoprotein. Proceedings of the National Academy of Sciences of the United States of America, 2018, 115, E8892-E8899.	7.1	72
36	Intra-seasonal antibody repertoire analysis of a subject immunized with an MF59®-adjuvanted pandemic 2009 H1N1 vaccine. Vaccine, 2018, 36, 5325-5332.	3.8	4

#	Article	IF	CITATIONS
37	How small-molecule inhibitors of dengue-virus infection interfere with viral membrane fusion. ELife, 2018, 7, .	6.0	16
38	Conformational States of a Soluble, Uncleaved HIV-1 Envelope Trimer. Journal of Virology, 2017, 91, .	3.4	19
39	Antigenicity-defined conformations of an extremely neutralization-resistant HIV-1 envelope spike. Proceedings of the National Academy of Sciences of the United States of America, 2017, 114, 4477-4482.	7.1	18
40	Protein tentacles. Journal of Structural Biology, 2017, 200, 244-247.	2.8	8
41	CryoEM Structure of an Influenza Virus Receptor-Binding Site Antibody–Antigen Interface. Journal of Molecular Biology, 2017, 429, 1829-1839.	4.2	21
42	Staged induction of HIV-1 glycan–dependent broadly neutralizing antibodies. Science Translational Medicine, 2017, 9, .	12.4	212
43	Mechanism of membrane fusion induced by vesicular stomatitis virus G protein. Proceedings of the National Academy of Sciences of the United States of America, 2017, 114, E28-E36.	7.1	98
44	The Kinetochore Receptor for the Cohesin Loading Complex. Cell, 2017, 171, 72-84.e13.	28.9	88
45	Single-Particle Detection of Transcription following Rotavirus Entry. Journal of Virology, 2017, 91, .	3.4	23
46	Pictures of the prologue to neurotransmitter release. Proceedings of the National Academy of Sciences of the United States of America, 2017, 114, 8920-8922.	7.1	3
47	Initiation of HIV neutralizing B cell lineages with sequential envelope immunizations. Nature Communications, 2017, 8, 1732.	12.8	76
48	Molecular Structures of Yeast Kinetochore Subcomplexes and Their Roles in Chromosome Segregation. Cold Spring Harbor Symposia on Quantitative Biology, 2017, 82, 83-89.	1.1	10
49	Boosting of HIV envelope CD4 binding site antibodies with long variable heavy third complementarity determining region in the randomized double blind RV305 HIV-1 vaccine trial. PLoS Pathogens, 2017, 13, e1006182.	4.7	38
50	Conserved Tetramer Junction in the Kinetochore Ndc80 Complex. Cell Reports, 2016, 17, 1915-1922.	6.4	51
51	Complex Antigens Drive Permissive Clonal Selection in Germinal Centers. Immunity, 2016, 44, 542-552.	14.3	278
52	Immunogenic cross-talk between dengue and Zika viruses. Nature Immunology, 2016, 17, 1010-1012.	14.5	34
53	Structure of the MIS12 Complex and Molecular Basis of Its Interaction with CENP-C at Human Kinetochores. Cell, 2016, 167, 1028-1040.e15.	28.9	126
54	Structure of the MIND Complex Defines a Regulatory Focus for Yeast Kinetochore Assembly. Cell, 2016, 167, 1014-1027.e12.	28.9	121

#	Article	IF	CITATIONS
55	Influenza immunization elicits antibodies specific for an egg-adapted vaccine strain. Nature Medicine, 2016, 22, 1465-1469.	30.7	104
56	Structural Constraints of Vaccine-Induced Tier-2 Autologous HIV Neutralizing Antibodies Targeting the Receptor-Binding Site. Cell Reports, 2016, 14, 43-54.	6.4	45
57	Immunogenic Stimulus for Germline Precursors of Antibodies that Engage the Influenza Hemagglutinin Receptor-Binding Site. Cell Reports, 2015, 13, 2842-2850.	6.4	67
58	Molecular Basis for Antibody-Mediated Neutralization of New World Hemorrhagic Fever Mammarenaviruses. Cell Host and Microbe, 2015, 18, 705-713.	11.0	44
59	Structure of the L Protein of Vesicular Stomatitis Virus from Electron Cryomicroscopy. Cell, 2015, 162, 314-327.	28.9	211
60	Viral Receptor-Binding Site Antibodies with Diverse Germline Origins. Cell, 2015, 161, 1026-1034.	28.9	151
61	Viral membrane fusion. Virology, 2015, 479-480, 498-507.	2.4	594
62	Key mutations stabilize antigenâ€binding conformation during affinity maturation of a broadly neutralizing influenza antibody lineage. Proteins: Structure, Function and Bioinformatics, 2015, 83, 771-780.	2.6	34
63	Veritas per structuram. Annual Review of Biochemistry, 2015, 84, 37-60.	11.1	1
64	Structural evidence for Scc4-dependent localization of cohesin loading. ELife, 2015, 4, e06057.	6.0	69
65	Autoinhibition of Bruton's tyrosine kinase (Btk) and activation by soluble inositol hexakisphosphate. ELife, 2015, 4, .	6.0	82
66	Distinct functional determinants of influenza hemagglutinin-mediated membrane fusion. ELife, 2015, 4, e11009.	6.0	53
67	Sequential conformational rearrangements in flavivirus membrane fusion. ELife, 2014, 3, e04389.	6.0	72
68	Structural Correlates of Rotavirus Cell Entry. PLoS Pathogens, 2014, 10, e1004355.	4.7	55
69	Affinity maturation in an HIV broadly neutralizing B-cell lineage through reorientation of variable domains. Proceedings of the National Academy of Sciences of the United States of America, 2014, 111, 10275-10280.	7.1	73
70	Stable, uncleaved HIV-1 envelope glycoprotein gp140 forms a tightly folded trimer with a native-like structure. Proceedings of the National Academy of Sciences of the United States of America, 2014, 111, 18542-18547.	7.1	67
71	An Iml3-Chl4 Heterodimer Links the Core Centromere to Factors Required for Accurate Chromosome Segregation. Cell Reports, 2013, 5, 29-36.	6.4	56
72	Structure of a Dengue Virus Envelope Protein Late-Stage Fusion Intermediate. Journal of Virology, 2013, 87, 2287-2293.	3.4	114

#	Article	IF	CITATIONS
73	Location of the dsRNA-Dependent Polymerase, VP1, in Rotavirus Particles. Journal of Molecular Biology, 2013, 425, 124-132.	4.2	69
74	Antigenicity and Immunogenicity of RV144 Vaccine AIDSVAX Clade E Envelope Immunogen Is Enhanced by a gp120 N-Terminal Deletion. Journal of Virology, 2013, 87, 1554-1568.	3.4	97
75	Preconfiguration of the antigen-binding site during affinity maturation of a broadly neutralizing influenza virus antibody. Proceedings of the National Academy of Sciences of the United States of America, 2013, 110, 264-269.	7.1	227
76	Influenza-virus membrane fusion by cooperative fold-back of stochastically induced hemagglutinin intermediates. ELife, 2013, 2, e00333.	6.0	154
77	Small-Molecule Inhibitors of Dengue-Virus Entry. PLoS Pathogens, 2012, 8, e1002627.	4.7	80
78	Ndc10 is a platform for inner kinetochore assembly in budding yeast. Nature Structural and Molecular Biology, 2012, 19, 48-55.	8.2	54
79	RWD domain: a recurring module in kinetochore architecture shown by a Ctf19–Mcm21 complex structure. EMBO Reports, 2012, 13, 216-222.	4.5	62
80	Beam-induced motion of vitrified specimen on holey carbon film. Journal of Structural Biology, 2012, 177, 630-637.	2.8	366
81	Molecular Architecture of the Yeast Monopolin Complex. Cell Reports, 2012, 1, 583-589.	6.4	46
82	B-cell–lineage immunogen design in vaccine development with HIV-1 as a case study. Nature Biotechnology, 2012, 30, 423-433.	17.5	432
83	Movies of Ice-Embedded Particles Enhance Resolution in Electron Cryo-Microscopy. Structure, 2012, 20, 1823-1828.	3.3	277
84	Kinetics of Proton Transport into Influenza Virions by the Viral M2 Channel. PLoS ONE, 2012, 7, e31566.	2.5	31
85	Single-molecule analysis of a molecular disassemblase reveals the mechanism of Hsc70-driven clathrin uncoating. Nature Structural and Molecular Biology, 2011, 18, 295-301.	8.2	101
86	Atomic model of an infectious rotavirus particle. EMBO Journal, 2011, 30, 408-416.	7.8	254
87	Near-atomic resolution reconstructions of icosahedral viruses from electron cryo-microscopy. Current Opinion in Structural Biology, 2011, 21, 265-273.	5.7	148
88	Broadly neutralizing human antibody that recognizes the receptor-binding pocket of influenza virus hemagglutinin. Proceedings of the National Academy of Sciences of the United States of America, 2011, 108, 14216-14221.	7.1	402
89	Recognition of the centromere-specific histone Cse4 by the chaperone Scm3. Proceedings of the National Academy of Sciences of the United States of America, 2011, 108, 9367-9371.	7.1	95
90	Cross-Linking of Rotavirus Outer Capsid Protein VP7 by Antibodies or Disulfides Inhibits Viral Entry. Journal of Virology, 2011, 85, 10509-10517.	3.4	24

#	Article	IF	CITATIONS
91	Structural basis for receptor recognition by New World hemorrhagic fever arenaviruses. Nature Structural and Molecular Biology, 2010, 17, 438-444.	8.2	125
92	Conservation in vesicle coats. Nature, 2010, 466, 1048-1049.	27.8	17
93	Peptide Inhibitors of Flavivirus Entry Derived from the E Protein Stem. Journal of Virology, 2010, 84, 12549-12554.	3.4	85
94	Effect of Mutations in VP5* Hydrophobic Loops on Rotavirus Cell Entry. Journal of Virology, 2010, 84, 6200-6207.	3.4	40
95	Peptide Inhibitors of Dengue-Virus Entry Target a Late-Stage Fusion Intermediate. PLoS Pathogens, 2010, 6, e1000851.	4.7	113
96	Mechanistic Biology in the Next Quarter Century. Molecular Biology of the Cell, 2010, 21, 3799-3800.	2.1	2
97	Looking Inside Adenovirus. Science, 2010, 329, 1026-1027.	12.6	34
98	X-ray Crystal Structure of the Rotavirus Inner Capsid Particle at 3.8ÂÃ Resolution. Journal of Molecular Biology, 2010, 397, 587-599.	4.2	124
99	The Monopolin Complex Crosslinks Kinetochore Components to Regulate Chromosome-Microtubule Attachments. Cell, 2010, 142, 556-567.	28.9	119
100	A Rotavirus Spike Protein Conformational Intermediate Binds Lipid Bilayers. Journal of Virology, 2010, 84, 1764-1770.	3.4	50
101	Subunit interactions in bovine papillomavirus. Proceedings of the National Academy of Sciences of the United States of America, 2010, 107, 6298-6303.	7.1	134
102	Structure of Rotavirus Outer-Layer Protein VP7 Bound with a Neutralizing Fab. Science, 2009, 324, 1444-1447.	12.6	216
103	Molecular interactions in rotavirus assembly and uncoating seen by high-resolution cryo-EM. Proceedings of the National Academy of Sciences of the United States of America, 2009, 106, 10644-10648.	7.1	135
104	VP5* Rearranges when Rotavirus Uncoats. Journal of Virology, 2009, 83, 11372-11377.	3.4	43
105	Requirements for the Formation of Membrane Pores by the Reovirus Myristoylated μ1N Peptide. Journal of Virology, 2009, 83, 7004-7014.	3.4	55
106	Role of HIV membrane in neutralization by two broadly neutralizing antibodies. Proceedings of the National Academy of Sciences of the United States of America, 2009, 106, 20234-20239.	7.1	225
107	Viral membrane fusion. Nature Structural and Molecular Biology, 2008, 15, 690-698.	8.2	1,060
108	Mechanism for Coordinated RNA Packaging and Genome Replication by Rotavirus Polymerase VP1. Structure, 2008, 16, 1678-1688.	3.3	148

#	Article	IF	CITATIONS
109	Single-particle kinetics of influenza virus membrane fusion. Proceedings of the National Academy of Sciences of the United States of America, 2008, 105, 15382-15387.	7.1	248
110	The pH sensor for flavivirus membrane fusion. Journal of Cell Biology, 2008, 183, 177-179.	5.2	39
111	Near-atomic resolution using electron cryomicroscopy and single-particle reconstruction. Proceedings of the National Academy of Sciences of the United States of America, 2008, 105, 1867-1872.	7.1	347
112	Structure and Function of an Essential Component of the Outer Membrane Protein Assembly Machine. Science, 2007, 317, 961-964.	12.6	327
113	Protein Arms in the Kinetochore-Microtubule Interface of the Yeast DASH Complex. Molecular Biology of the Cell, 2007, 18, 2503-2510.	2.1	55
114	An Atomic Model of the Interferon-Î ² Enhanceosome. Cell, 2007, 129, 1111-1123.	28.9	547
115	The Ndc80/HEC1 complex is a contact point for kinetochore-microtubule attachment. Nature Structural and Molecular Biology, 2007, 14, 54-59.	8.2	307
116	Three-dimensional intricacies in protein-DNA recognition and transcriptional control. Nature Structural and Molecular Biology, 2007, 14, 1118-1119.	8.2	5
117	Comments on the NIGMS PSI. Structure, 2007, 15, 1344-1346.	3.3	8
118	Single Particle Reconstructions of the Transferrin–Transferrin Receptor Complex Obtained with Different Specimen Preparation Techniques. Journal of Molecular Biology, 2006, 355, 1048-1065.	4.2	57
119	PL-6 Structure of the aquaporin-0 mediated membrane junction(Plenary Lecture,Abstract,Meeting) Tj ETQq1 1 0.	.784314 rg 0.1	gBT /Overlock
120	Structure of a Central Component of the Yeast Kinetochore: The Spc24p/Spc25p Globular Domain. Structure, 2006, 14, 1003-1009.	3.3	86
121	Small molecules that bind the inner core of gp41 and inhibit HIV envelope-mediated fusion. Proceedings of the National Academy of Sciences of the United States of America, 2006, 103, 13938-13943.	7.1	133
122	Stu2p binds tubulin and undergoes an open-to-closed conformational change. Journal of Cell Biology, 2006, 172, 1009-1022.	5.2	119
123	Crystal Structure of Glycoprotein B from Herpes Simplex Virus 1. Science, 2006, 313, 217-220.	12.6	493
124	The yeast DASH complex forms closed rings on microtubules. Nature Structural and Molecular Biology, 2005, 12, 138-143.	8.2	258
125	Structure of an unliganded simian immunodeficiency virus gp120 core. Nature, 2005, 433, 834-841.	27.8	483
126	Features of Reovirus Outer Capsid Protein μ1 Revealed by Electron Cryomicroscopy and Image Reconstruction of the Virion at 7.0 Ã Resolution. Structure, 2005, 13, 1545-1557.	3.3	80

#	Article	IF	CITATIONS
127	Molecular organization of the Ndc80 complex, an essential kinetochore component. Proceedings of the National Academy of Sciences of the United States of America, 2005, 102, 5363-5367.	7.1	243
128	Mechanism of Membrane Fusion by Viral Envelope Proteins. Advances in Virus Research, 2005, 64, 231-261.	2.1	162
129	Perspective: Discovery of antivirals against smallpox. Proceedings of the National Academy of Sciences of the United States of America, 2004, 101, 11178-11192.	7.1	93
130	Crystal structure of ATF-2/c-Jun and IRF-3 bound to the interferon-β enhancer. EMBO Journal, 2004, 23, 4384-4393.	7.8	156
131	Whither structural biology?. Nature Structural and Molecular Biology, 2004, 11, 12-15.	8.2	64
132	Structure of the dengue virus envelope protein after membrane fusion. Nature, 2004, 427, 313-319.	27.8	995
133	X-ray structure of a protein-conducting channel. Nature, 2004, 427, 36-44.	27.8	1,134
134	Structural rearrangements in the membrane penetration protein of a non-enveloped virus. Nature, 2004, 430, 1053-1058.	27.8	200
135	Molecular model for a complete clathrin lattice from electron cryomicroscopy. Nature, 2004, 432, 573-579.	27.8	464
136	Structure of the Human Transferrin Receptor-Transferrin Complex. Cell, 2004, 116, 565-576.	28.9	475
137	Two Distinct Size Classes of Immature and Mature Subviral Particles from Tick-Borne Encephalitis Virus. Journal of Virology, 2003, 77, 11357-11366.	3.4	69
138	Variation on an Src-like Theme. Cell, 2003, 112, 737-740.	28.9	173
139	A ligand-binding pocket in the dengue virus envelope glycoprotein. Proceedings of the National Academy of Sciences of the United States of America, 2003, 100, 6986-6991.	7.1	927
140	Specificity and Affinity of Sialic Acid Binding by the Rhesus Rotavirus VP8* Core. Journal of Virology, 2002, 76, 10512-10517.	3.4	68
141	The rhesus rotavirus VP4 sialic acid binding domain has a galectin fold with a novel carbohydrate binding site. EMBO Journal, 2002, 21, 885-897.	7.8	305
142	Structure of the Reovirus Membrane-Penetration Protein, \hat{l} /41, in a Complex with Its Protector Protein, \hat{l} f3. Cell, 2002, 108, 283-295.	28.9	225
143	Don C. Wiley (1944–2001). Cell, 2002, 108, 313-315.	28.9	2
144	RNA Synthesis in a Cage—Structural Studies of Reovirus Polymerase λ3. Cell, 2002, 111, 733-745.	28.9	309

#	Article	IF	CITATIONS
145	Don C. Wiley (1944–2001). Molecular Cell, 2002, 9, 225-227.	9.7	Ο
146	Atomic model of the papillomavirus capsid. EMBO Journal, 2002, 21, 4754-4762.	7.8	232
147	Molecular Organization of a Recombinant Subviral Particle from Tick-Borne Encephalitis Virus. Molecular Cell, 2001, 7, 593-602.	9.7	240
148	Structure of the reovirus core at 3.6?Ã resolution. Nature, 2000, 404, 960-967.	27.8	428
149	Purified Recombinant Rotavirus VP7 Forms Soluble, Calcium-Dependent Trimers. Virology, 2000, 277, 420-428.	2.4	62
150	Structure of Small Virus-like Particles Assembled from the L1 Protein of Human Papillomavirus 16. Molecular Cell, 2000, 5, 557-567.	9.7	417
151	Structure of PAK1 in an Autoinhibited Conformation Reveals a Multistage Activation Switch. Cell, 2000, 102, 387-397.	28.9	481
152	Selection of gp41-mediated HIV-1 cell entry inhibitors from biased combinatorial libraries of non-natural binding elements. Nature Structural Biology, 1999, 6, 953-960.	9.7	140
153	Crystal Structures of c-Src Reveal Features of Its Autoinhibitory Mechanism. Molecular Cell, 1999, 3, 629-638.	9.7	786
154	Atomic Structure of Clathrin. Cell, 1998, 95, 563-573.	28.9	217
155	Structure of a Covalently Trapped Catalytic Complex of HIV-1 Reverse Transcriptase: Implications for Drug Resistance. Science, 1998, 282, 1669-1675.	12.6	1,317
156	Three-dimensional structure of the tyrosine kinase c-Src. Nature, 1997, 385, 595-602.	27.8	1,386
157	Crystal structure of ICAM-2 reveals a distinctive integrin recognition surface. Nature, 1997, 387, 312-315.	27.8	115
158	Peptide–Surface Association: The Case of PDZ and PTB Domains. Cell, 1996, 86, 341-343.	28.9	170
159	Phosphorylated T Cell Receptor zeta-chain and ZAP70 Tandem SH2 Domains form a 1:3 Complex in vitro. FEBS Journal, 1996, 238, 440-445.	0.2	26
160	Crystal structures of murine polyomavirus in complex with straight-chain and branched-chain sialyloligosaccharide receptor fragments. Structure, 1996, 4, 183-194.	3.3	172
161	Retrovirus envelope domain at 1.7 Ã resolution. Nature Structural Biology, 1996, 3, 465-469.	9.7	328
162	Structure and mechanism of DNA topoisomerase II. Nature, 1996, 379, 225-232.	27.8	813

#	Article	IF	CITATIONS
163	Spatial constraints on the recognition of phosphoproteins by the tandem SH2 domains of the phosphatase SH-PTP2. Nature, 1996, 379, 277-280.	27.8	192
164	Varmus at Harvard. Science, 1996, 273, 413-413.	12.6	0
165	Crystal structure of the heterodimeric bZIP transcription factor c-Fos–c-Jun bound to DNA. Nature, 1995, 373, 257-261.	27.8	736
166	Structure of the NF- \hat{I}^{0} B p50 homodimer bound to DNA. Nature, 1995, 373, 311-317.	27.8	531
167	The envelope glycoprotein from tick-borne encephalitis virus at 2 Ã resolution. Nature, 1995, 375, 291-298.	27.8	1,344
168	Structure of murine polyomavirus complexed with an oligosaccharide receptor fragment. Nature, 1994, 369, 160-163.	27.8	307
169	Recognition of a high-affinity phosphotyrosyl peptide by the Src homology-2 domain of p56lck. Nature, 1993, 362, 87-91.	27.8	545
170	The GCN4 basic region leucine zipper binds DNA as a dimer of uninterrupted α Helices: Crystal structure of the protein-DNA complex. Cell, 1992, 71, 1223-1237.	28.9	1,035
171	DNA recognition by GAL4: structure of a protein-DNA complex. Nature, 1992, 356, 408-414.	27.8	685
172	Solution structure of the DNA-binding domain of Cd2-GAL4 from S. cerevisiae. Nature, 1992, 356, 450-453.	27.8	134
173	A structural taxonomy of DNA-binding domains. Nature, 1991, 353, 715-719.	27.8	672
174	Folding transition in the DMA-binding domain of GCN4 on specific binding to DNA. Nature, 1990, 347, 575-578.	27.8	418
175	Atomic structure of a fragment of human CD4 containing two immunoglobulin-like domains. Nature, 1990, 348, 411-418.	27.8	610
176	Structure of a phage 434 Cro/DNA complex. Nature, 1988, 335, 789-795.	27.8	211
177	Effect of non-contacted bases on the affinity of 434 operator for 434 repressor and Cro. Nature, 1987, 326, 886-888.	27.8	235
178	Protein structures: Two for the price of one. Nature, 1985, 313, 736-737.	27.8	6
179	A phage repressor–operator complex at 7 à resolution. Nature, 1985, 316, 596-601.	27.8	143
180	Virus structure: First comparison of two animal viruses in three dimensions. Nature, 1985, 317, 382-383.	27.8	4

#	Article	IF	CITATIONS
181	X-ray crystallography: Advantages of electronic â€~film'. Nature, 1984, 309, 408-408.	27.8	4
182	Assembly of the head of bacteriophage P22: X-ray diffraction from heads, proheads and related structures. Journal of Molecular Biology, 1976, 104, 387-410.	4.2	209